Journal of Bone and Mineral Metabolism (2019) 37:614–626
https://doi.org/10.1007/s00774-018-0963-7

ORIGINAL ARTICLE

Screening of key candidate genes and pathways for osteocytes involved in the differential response to different types of mechanical stimulation using a bioinformatics analysis

Ziyi Wang[1] · Yoshihito Ishihara[2] · Takanori Ishikawa[2] · Mitsuhiro Hoshijima[1] · Naoya Odagaki[2] · Ei Ei Hsu Hlaing[1] · Hiroshi Kamioka[1]

Received: 15 January 2018 / Accepted: 25 September 2018 / Published online: 9 November 2018

Abstract

This study aimed to predict the key genes and pathways that are activated when different types of mechanical loading are applied to osteocytes. mRNA expression datasets (series number of GSE62128 and GSE42874) were obtained from Gene Expression Omnibus database (GEO). High gravity-treated osteocytic MLO-Y4 cell-line samples from GSE62128 (Set1), and fluid flow-treated MLO-Y4 samples from GSE42874 (Set2) were employed. After identifying the differentially expressed genes (DEGs), functional enrichment was performed. The common DEGs between Set1 and Set2 were considered as key DEGs, then a protein–protein interaction (PPI) network was constructed using the minimal nodes from all of the DEGs in Set1 and Set2, which linked most of the key DEGs. Several open source software programs were employed to process and analyze the original data. The bioinformatic results and the biological meaning were validated by in vitro experiments. High gravity and fluid flow induced opposite expression trends in the key DEGs. The hypoxia-related biological process and signaling pathway were the common functional enrichment terms among the DEGs from Set1, Set2 and the PPI network. The expression of almost all the key DEGs (*Pdk1*, *Ccng2*, *Eno2*, *Egln1*, *Higd1a*, *Slc5a3* and *Mxi1*) were mechano-sensitive. Eno2 was identified as the hub gene in the PPI network. *Eno2* knockdown results in expression changes of some other key DEGs (*Pdk1*, *Mxi1* and *Higd1a*). Our findings indicated that the hypoxia response might have an important role in the differential responses of osteocytes to the different types of mechanical force.

Keywords Osteocyte · Mechanical stimulation · Bioinformatics analysis · Microarray · Fluid flow

Introduction

More than a century ago, we already knew that the trabecular structure of bone was closely related to its mechanical loading (Wolff's Law). It seems that bone cells can sense the different force-direction, force-strength and force-type and respond to them differentially. In vivo, osteocytes are usually influenced by several forces, including body forces (e.g., gravity) and surface forces (fluid shear stress, tensile and compressive stress), which are applied in different directions or with different strength. A body force acts throughout the volume of a body and will cause an object to accelerate, which contrasts with surface force, which is exerted on the surface of an object. The elucidation of the mechanisms underlying these phenomena may be important for understanding the regulation of bone remodeling by a locally acting mechanical force. Bone remodeling is a dynamic process that involves a delicate equilibrium between the function of osteoblasts and osteoclasts. However, research has shown that other cells are involved in this process, most notably osteocytes, which are now considered to be essential players in the process through which the bone senses different types of mechanical force (e.g., pressure, tension, fluid flow and shear stress, etc.) [1]. The clarification of the mechanism

Electronic supplementary material The online version of this article (https://doi.org/10.1007/s00774-018-0963-7) contains supplementary material, which is available to authorized users.

✉ Hiroshi Kamioka
kamioka@md.okayama-u.ac.jp

[1] Department of Orthodontics, Okayama University Graduate School of Medicine, Dentistry, and Pharmaceutical Sciences, 2-5-1 Shikata, Kita-ku, Okayama 700-8525, Japan

[2] Department of Orthodontics, Okayama University Hospital, Okayama, Japan

underlying the differential responses of bone to various mechanical stimuli is very important for developing novel therapeutic approaches to bone diseases.

Osteocytes, cells with a stellate shape and which are embedded into the mineralized bone tissue, are the most abundant cells in the bone. They are connected with each other via a cellular network formed by their cytoplasmic processes. This osteocyte network has long been thought to play a central role in regulating bone modeling and remodeling by detecting mechanical stimuli to the skeleton through interstitial fluid flow [2, 3] or deformation of the cell body [4]. It is also known that osteocytes are able to orchestrate the function of osteoblasts and osteoclasts [5, 6]. In particular, a previous study reported that osteocytes but not bone surface cells (osteoblasts, osteoclasts, etc.), responded to dynamic mechanical loading in the long bones with multiple Ca^{2+} spikes [7].

We hypothesized that osteocytes may be an essential part of the process through which bone differentially responds to various types of mechanical stimuli. To test this hypothesis, we screened the differentially expressed genes (DEGs) of the datasets from the Gene Expression Omnibus (GEO) database to investigate the mechanism underlying this process. GSE62128 and GSE42874, which exposed MLO-Y4 to different types of mechanical stimuli, were used to screen out the key DEGs for further examination in a functional and pathway enrichment analysis. Finally, the expression levels of key DEGs were validated by several in vitro experiments (See a work flow of this study in Online Resource 1.

Materials and methods

Acquisition of microarray data

The raw data with CEL files of three 2-fold gravity of Earth-treated (performed using a large-gradient, high-magnetic-field) (GSM1520101, GSM1520102, GSM1520103) and three gravity of Earth-treated (GSM1520104, GSM1520105, GSM1520106) murine long bone osteocyte Y4 (MLO-Y4) samples of GSE62128 (Set 1), and the raw data with CEL files of three 2-h fluid flow-treated (GSM1052656, GSM1052657, GSM1052658) and 2-h sham-treated (GSM1052653, GSM1052654, GSM1052655) MLO-Y4 samples of GSE42874 (Set 2) were obtained from the Gene Expression Omnibus (GEO) (http://www.ncbi.nlm.nih.gov/geo/).

Identification of differently expressed genes (DEGs)

The screening threshold was a false discovery rate (FDR) corrected P value of < 0.1 (also known as the q-value) and a $|\log_2^{\text{Fold Change}}|$ value of > 0.59 (2-fold increase or 50% decrease). The raw data with the CEL files of Set1 and Set2 were background corrected, normalized, annotated and $\log_2$ transformed using the xps package (https://bioconductor.org/packages/release/bioc/html/xps.html) in *R*. Empirical Bayes statistical tests using moderated genewise variance were performed using the limma package [8] for *R*. If multiple probes correspond to one gene, only the most significant (smaller q-value) result is kept. The DEGs were then identified according to the criteria of a $|\log_2^{\text{Fold Change}}|$ value of > 0.59 and a q-value of < 0.1. The common DEGs between Set1 and Set2 were considered as the key DEGs.

Scripts written in the *R* programming language to allow all of the above-described data processing procedures and detailed instructions to allow for the reproduction of our results are available from GitHub (https://github.com/wong-ziyi/Microarray_Analysis).

The biological function and pathway enrichment analysis of DEGs from Set1 and Set2

To investigate the functional difference when different mechanical forces are applied, biological function and pathway enrichment analyses were performed for Set1 and Set2. Gene Ontology (GO; http://www.geneontology.org) [9, 10] is a tool used for the unification of biological functions based on gene annotation information, which primarily consists of biological process (BP), molecular function (MF), and cellular component (CC) analyses. The Kyoto Encyclopedia of Genes and Genomes (KEGG; available at http://www.genome.ad.jp/kegg/) [11] is a pathway-associated database that connects known information on molecular interaction networks. To understand the biological significance of the identified DEGs, the upregulated DEGs of Set1, the downregulated DEGs of Set1, the upregulated DEGs of Set2 and the downregulated DEGs of Set2 were separately input into the Database for Annotation Visualization and Integrated Discovery (DAVID; http://david.abcc.ncifcrf.gov/) [12] for the GO term and KEGG pathway analyses. An EASE Score (a modified Fisher's exact P value) of < 0.01 and a gene count of > 2 were considered to indicate a statistically significant difference. The common functional terms or the KEGG pathways between Set1 and Set2 were considered to be the key biological process and pathways.

PPI network construction

The Search Tool for the Retrieval of Interacting Genes database (STRING) [13] database (https://string-db.org/) provides comprehensive information on the functional interactions between DEGs by calculating their combined score. Using a minimum required interaction score of 0.15 (low confidence), PPI networks were constructed based on the PPI pairs from the key candidate DEGs and the remaining

308 DEGs (Fig. 1) from Set1 and Set2 using the Cytoscape software program (version 3.6.0) (available at http://cytoscapeweb.cytoscape.org/) [14]. Then Pesca 3.0 (a Cytoscape software application) was applied to screen out a subnetwork that was constructed using the minimal nodes linking all key candidate DEGs. Finally, we retrieved the KEGG enrichment of this subnetwork in the Cytoscape software program using the STRING enrichment application programming interface (API). We analyzed the topological properties of this subnetwork using the tYNA web interface (http://tyna.gersteinlab.org/) [15]. In the nodes with a degree that was greater than or equal to the sum of the mean and the standard deviation (SD), the one that has highest mean interaction score was selected as a key hub gene. STRING also allows users to retrieve the functional enrichment (GO terms and KEGG pathway). The significant functional enrichment terms were identified according the criterion of FDR < 0.05.

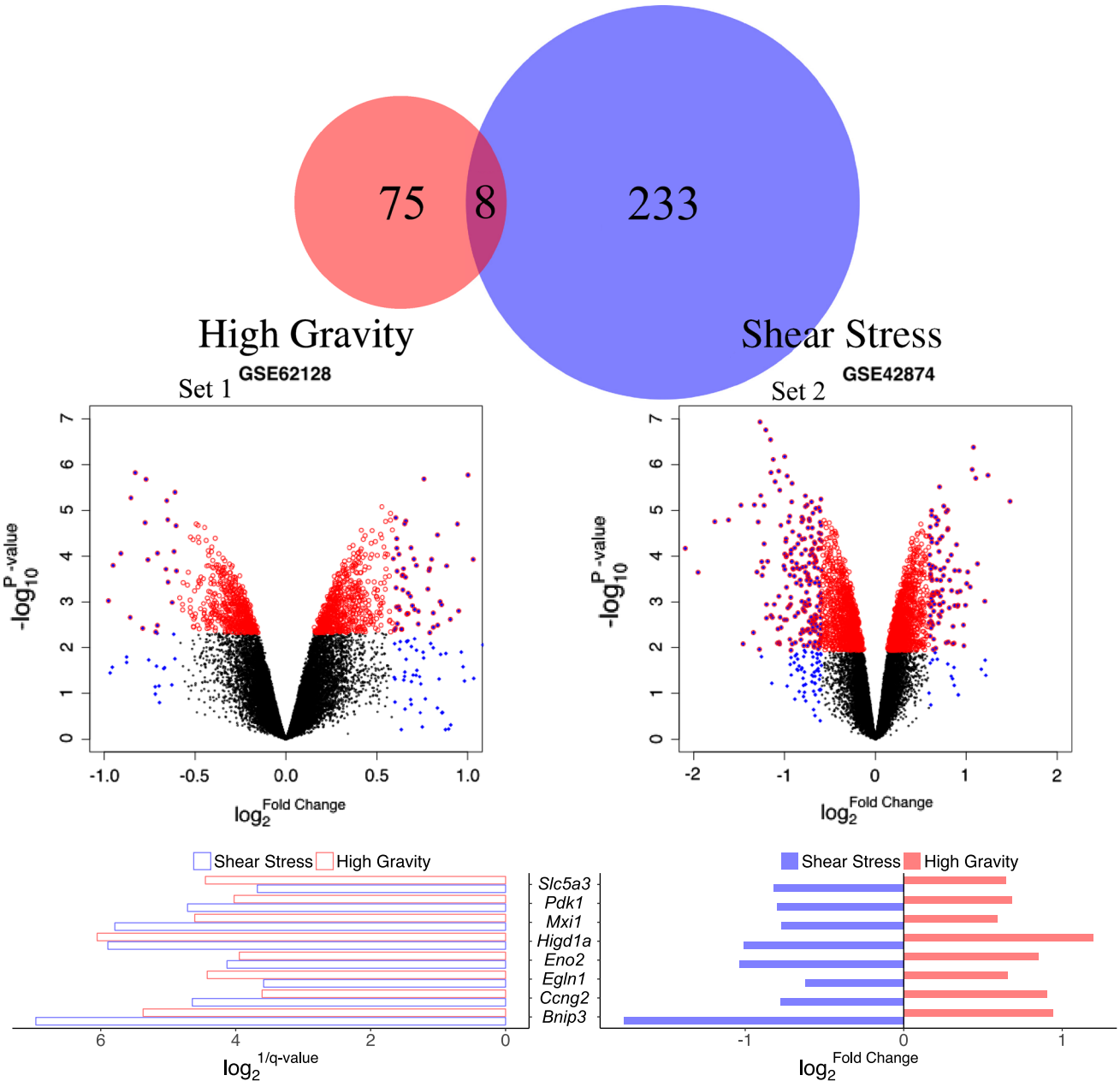

Fig. 1 Overview of the DEGs from Set1 and Set2. The significance and the expression levels of the common DEGs in these two datasets are shown in the bottom panel. The expression levels of the common DEGs showed totally opposite trends in Set1 and Set2

Fluid flow exposed osteocytic MLO-Y4 cells

The design we employed was described in our previous study [16]. Briefly, the cells were subjected to fluid flow in a parallel plate flow chamber (Waken Denshi Co.) connected to a flow loop apparatus that was modified from the apparatus described by Frangos et al. [17] to accept quartz glass microscope slides. Osteocytic MLO-Y4 cells were cultured on collagen I-coated glass slides in α-modified Minimum Essential Medium (α-MEM; Invitrogen) with 5.0% heat-inactivated fetal bovine serum (HIFBS; HyClone) and 5.0% bovine calf serum (BCS; HyClone) and antibiotics for 2 days and then exposed for 2 h to sinusoidally oscillating fluid flow in parallel plate flow chambers, inducing 2.5 dyn/cm^2 or 50 dyn/cm^2 shear stress. Paired sham controls were maintained on the same glass slides.

Compressed osteocytic MLO-Y4 cells

As described in our previous study [18], osteocytic MLO-Y4 cells were cultured on collagen I-coated glass plates that were maintained in 6-well plates in α-MEM with 5.0% HIFBS and 5.0% BCS and antibiotics for 2 days and then exposed (by direct contact) for 2 h to weights (0.051 g/cm^2), inducing 50 dyn/cm^2 of continuous compression force.

Eno2 gene silencing by the siRNA

Eno2 siRNA (Mission® siRNA select SASI_Mm01_00106092) and negative control siRNA (Mission® siRNA select Mission_Negative control SIC_001) were purchased from Merck (Germany). siRNA was delivered into the cells by electroporation using an Amaxa™ Human Chondrocyte Nucleofector™ kit and an Amaxa Nucleofector® II (Lonza Cologne GmbH, Cologne, Germany) according to the manufacturer's instructions. In brief, 4.0×10^5 MLO-Y4 cells were transfected with 100 nM siRNAs in the solution for electroporation (Nucleofector solution and supplement: 100 μL) using electroporation program U-024. Next, cells in α-MEM supplemented with 5% HIFBS and 5% BCS were seeded at a density of 4.0×10^5 cells/well into a six-well plate for RNA extraction and incubated at 37 °C under 5% CO_2 in air. After 48 h, the cells were collected for subsequent analyses.

Quantitative real-time reverse transcription-PCR (RT-PCR)

ISOGEN (Nippon Gene) and a ReverTra Ace qPCR RT Kit (Toyobo) were used to extract total RNA and to synthesize complementary DNA (cDNA), respectively. The resulting cDNA products were used as a template to quantify the relative content of messenger RNA (mRNA) by a quantitative real-time reverse transcription-PCR (RT-PCR). The relative levels of the PCR products were determined using a LightCycler System (Roche Diagnostics). SYBR green chemistry was used to determine the mRNA levels of the key DEGs and GAPDH, a housekeeping gene, in MLO-Y4 cells. The primers showed in Online Resource 2 were used.

Statistical analysis

A one-way analysis of variance (ANOVA) with the Holm–Sidak post hoc test was used to identify the statistical significance of the results from cells exposed to different force-direction or force-strength. An unpaired *t* test was used to compare the differentially expressed genes under hub gene knock-down. Pearson correlation test was applied to investigate the correlation between the hub gene and other target genes.

Results

The differential expression analysis

Gene expression profile Set1 (from GSE62128) and Set2 (from GSE42874) identified 83 and 241 DEGs, respectively (Fig. 1, see the entire list in the Online Resource 3 and 4). The common DEGs (*Slc5a3, Pdk1, Mxi1, Higd1a, Eno2, Egln1* and *Bnip3*) across Set 1 and Set 2 were taken as key DEGs. Notably, all key DEGs showed opposite expression trends between Set1 and Set2 (Fig. 1, right side on the bottom panel).

The functional and KEGG pathway enrichment analysis of DEGs from Set1 and Set2

The upregulated DEGs from Set1 and the downregulated DEGs from Set2 that were enriched in the same BP and KEGG terms were mainly associated with the response to hypoxia (Fig. 1). The entire functional enrichment terms are listed in Online Resources 5 and 6 for Set1 and Set2, respectively.

The PPI network and the corresponding KEGG pathway enrichment analysis

The PPI network generated from the DEGs of both Set1 and Set2 included a total of 298 nodes and 2476 edges (Online Resource 7). Then a subnetwork was constructed by the minimal nodes linking the most key candidate DEGs (Egln1, Eno2, Pdk1, Bnip3, Ccng2, Mxi1, Higd1a and Slc5a3). This

subnetwork contained a total of 9 nodes and 9 edges; the enriched BP and KEGG terms were mainly associated with the response to hypoxia (Fig. 3). Eno2 with a degree of 3 and a mean interaction score of 0.53 was selected as the hub gene (Fig. 3).

Verification of the mechano-sensitive expression and biological meaning of the key DEGs

The RT-PCR revealed that among the key DEGs, the expression of *Slc5a3*, *Pdk*, *Mxi1*, *Higd1a*, *Eno2*, and *Egln1* was mechano-sensitive. In addition, all of these genes showed response to a change of the force-strength of shear stress or a change of the force-direction. These genes showed more mechano-sensitivity than the *RANKL*/*OPG* ratio (Fig. 4). *Eno2* knockdown resulted in a significant increase in the expression of *Pdk1* and *Gap43*, and a significant decrease in the expression of *Higd1a* and *Mxi1* (Fig. 5a). A heatmap that was converted from the results showed in Figs. 4, 5b with a Pearson correlation test together to investigate the correlation of the Eno2 and expression of other genes (Pdk1, Higd1a, Mxi1, and Gap43) under different force-direction or force-strength conditions (Fig. 6). Figure 6 showed a significant positive correlation between the expression of *Eno2* and *Mxi1*. Although no significant correlation between the expression of *Eno2* and *Gap43*/*Higd1a* was observed in cells subjected to < 2.5 dyn/cm^2 in mechanical force, a strong and significant negative correlation (Fig. 6) was observed under extreme high mechanical force (50 dyn/cm^2). However, we did not observe any significant correlation between the expression of *Eno2* and *Pdk1*.

Discussion

The present study aimed to screen out the key candidate genes and pathways in osteocytes during the application of different types of mechanical stimuli (high gravity and shear force). We screened out eight common DEGs (*Slc5a3, Pdk1, Mxi1, Higd1a, Eno2, Egln1* and *Bnip3*) across Set1 and Set2, which were selected as candidate key DEGs for further investigation. The functional enrichment indicated that the biological processes related to the response to hypoxia and the HIF-1 signaling pathway had important roles in the mechano-transduction of osteocytes.

The mechano-sensitive expression of the key candidate DEGs

High gravity and shear force had an opposite influence on all of the key DEGs (Fig. 1, downregulated by high gravity and upregulated by shear force), which suggested that the osteocytes could sense and recognize different types of mechanical stimuli. To validate this finding from the microarray data, we investigated the expression of these key DEGs in MLO-Y4 osteocytes during shear stress under different conditions of force-strength or force-direction.

The RT-PCR revealed that, with the exception of *Bnip3*, the expression of the rest of the key DEGs in response to mechanical stress with a different force-strength or force-direction was mechano-sensitive (Fig. 4). Notably, the expression of *Pdk1*, *Ccng2*, *Eno2* and *Higd1a* showed opposite trends in response to a different force-direction (Fig. 4, compression vs shear stress under 50 dyn/cm^2) which is similar to the results revealed by microarray data, in which the expression showed opposite trends in response to shear stress and high gravity (Fig. 2). Eno2, the hub gene that was suggested by the subnetwork (Fig. 3), also showed more sensitivity to the mechanical force than other key DEGs (Fig. 4). On the other hand, *Eno2* knockdown results in significant expression changes of other three key DEGs (*Pdk1*, *Higd1a*, and *Mxi1*; see in Fig. 5a), and co-expression pattern between *Eno2* and *Mxi1*/*Higd1a* (Fig. 6). These results suggested that Eno2 might play a center role in the mechano-transduction of osteocytes to link the key DEGs.

Mechanical loading has been reported to create tears in the cell membrane called plasma membrane disruptions (PMDs) [19]. In that study, shear stress of 30 dyn/cm^2 created PMDs in more than 30% of osteocytes, while shear stress of 10 dyn/cm^2 created PMDs in less than 5% of osteocytes in vitro. Thus, in the present study, shear stress of 2.5 dyn/cm^2 and 50 dyn/cm^2 were defined as extremely low and extremely high mechanical force, respectively. Even under extremely low shear stress (2.5 dyn/cm^2), the expression levels of *Pdk1*, *Eno2*, *Egln1*, *Mxi1*, *RANKL*, *OPG*, and *RANKL*/*OPG* ratio showed significant changes. Moreover, the force-strength change of shear stress from 2.5 dyn/cm^2 to 50 dyn/cm^2 also induced significant changes in the expression of *Pdk1*, *Ccng2*, *Eno2*, *Egln1*, *Higd1a*, *Slc5a3*, and *Mxi1*, but not *RANKL*, *OPG*, and the *RANKL*/*OPG* ratio. Similarly, the force-direction change from shear force to compression induced significant changes in the expression of *Pdk1*, *Ccng2*, *Eno2*, *Higd1a*, *Slc5a3*, and *RANKL* but not *OPG* or the *RANKL*/*OPG* ratio (Fig. 4). These results indicated that the expression of *Slc5a3*, *Pdk1*, *Mxi1*, *Higd1a*, *Eno2*, and *Egln1* is more mechano-sensitive than that of *RANKL* and *OPG*.

Intriguingly, most of these mechano-sensitive genes (Egln1, Pdk1, Mxi1, and Slc5a3) clearly showed roles in bone development, modeling and remodeling—especially Egln1 and Pdk1, mechano-sensitive genes that are related to the hypoxic response (Fig. 3).

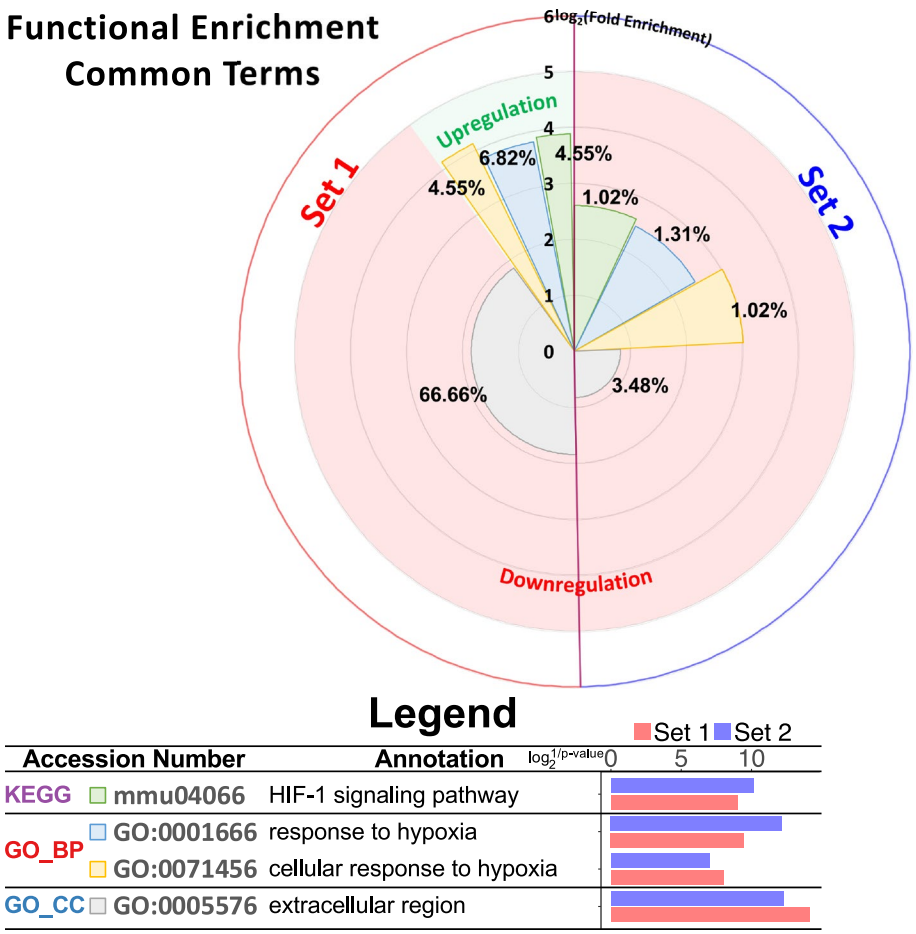

Fig. 2 Common functional enrichment terms in Set1 and Set2. In this rose plot, the height of each slice represented the $\log_2$ (fold enrichment) value. The radian of each slice represented the percentage of the DEGs covering the corresponding term in relation to all queried DEGs; the exact percentage is shown on the label of each slice. A red background indicates that the terms came from downregulated DEGs. A green background indicates that the terms came from upregulated DEGs. The entire list of the enrichment terms from Set1 and Set2 is shown in Online Resources 5 and 6

A potential key pathway through which various types of mechanical stimulation are recognized in osteocytes

Hypoxia-inducible transcription factor (HIF), is one of the key factors in the regulation of the function of osteoclasts and osteoblasts. The HIF heterodimer is composed of an inducible alpha subunit (HIF-1α, HIF-2α) and a constitutively expressed beta subunit (HIF-β/ARNT). Egl nine homolog 1 (Egln1), which is also known as prolyl-4-hydroxylase (PHD) domain-containing protein 1, is one of the PHD enzymes (PHD1-3). PHD enzymes, as a type of proteasome, degrade the HIF-α by hydroxylation, which results in the post-translational regulation of HIF. Previous studies have shown that the combined osteoblast-specific deletion of Egln2 with either Egln1 and/or Egln3 increased trabecular bone formation [20]. Similarly, the stabilization of HIF by inhibitors of PHD enzyme improved fracture healing, increased the bone mineral density and bone strength in murine models of bone fracture [21–24], distraction osteogenesis [25], and osteoporosis [26, 27].

On the other hand, the induction of pyruvate dehydrogenase kinase 1, the protein encoded by Pdk1, is directly regulated by HIF-1α, which in turn inhibits the activity of pyruvate dehydrogenase and thereby blocks the mitochondrial tricarboxylic acid cycle (TAC). As a consequence, the activity of HIF-1α could reduce the collagen hydroxylation, which was reported by a previous study [28]. Notably, HIF1 could directly regulate the expression of the Pdk1 gene in both humans [29, 30] and mice [28] by binding to several HIF1 consensus binding sites (also known as hypoxia response elements). The important role of the HIF-1 signal pathway in bone development, modeling and remodeling is well documented. However, its role in osteocyte function remains unclear. Our findings showed that the expression of both Egln1 and Pdk1 were mechano-sensitive. Moreover, the increased expression of *Pdk1* after *Eno2* knockdown suggested a novel potential pathway for regulation of *Pdk1* by *Eno2*. Taken together, our study suggested that the HIF-1 signal pathway is also important for mechano-transduction in osteocytes, and Eno2 may be involved in the regulation of HIF-1 signal pathway in osteocytes. The role of HIF-1 signal pathway in the osteocyte function is worthy of further study.

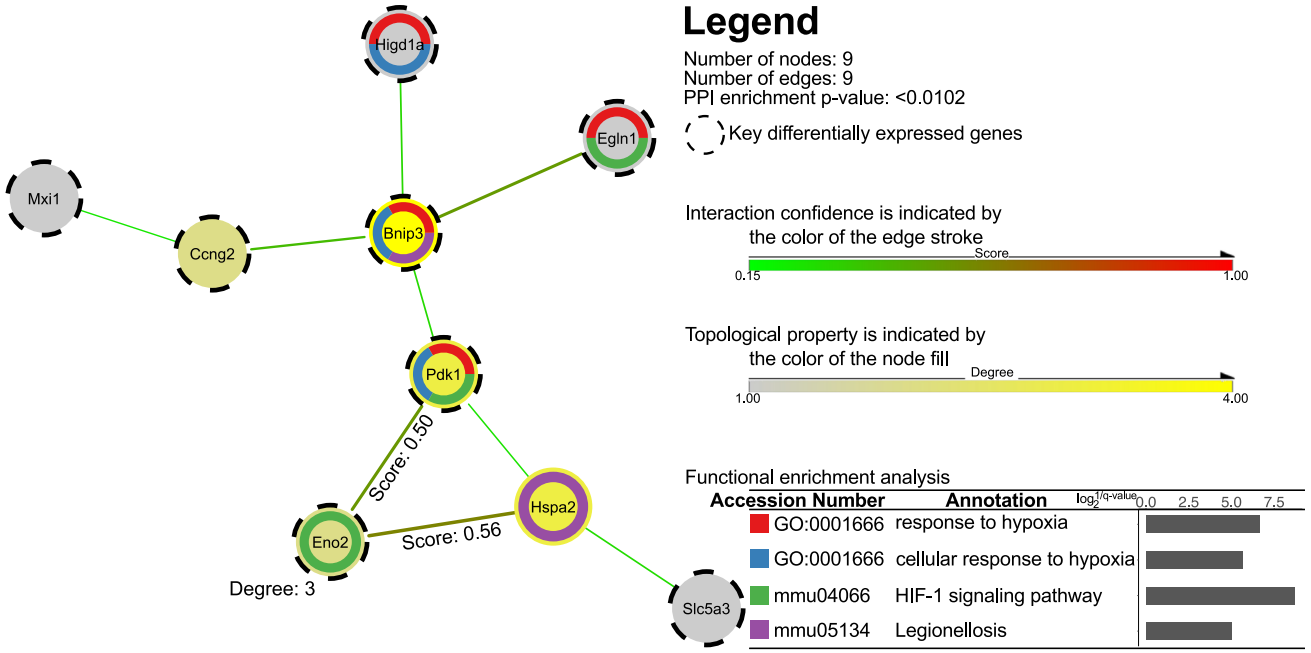

Fig. 3 The final PPI network was a sub-network (bottom panel) linking all of the key candidate DEGs from the origin network in Online Resource 7. This subnetwork contains 9 nodes and 9 edges with enrichment *P* value of < 0.0102. In this subnetwork, the interaction confidence is indicated by the color of edge stroke and the topological property is indicated by the color of the node fill. Eno2 with the degree of 3 and mean interaction confidence of 0.53 was identified as the hub gene. The functional enrichment terms were mainly related to the hypoxic response

Previous studies about the role of Mxi1, Slc5a3, Bnip3, Eno2, and Higd1a in bone

Besides Egln1 and Pdk1, other key DEGs were also found to play an important role in the bone metabolism.

Mxi1 encodes max-interacting protein 1, a transcription factor, was shown to suppress SOST transcription in human dermal fibroblasts in a recent study [31]. Sclerostin, which is encoded by SOST, a secretory protein that is specifically produced by osteocytes, suppresses osteogenesis by inhibiting WNT signaling [32, 33]. Recently, numerous studies have shown that sclerostin is a key determinant of the bone mass and a neutralizing antibody against sclerostin is currently being explored as a new therapeutic target for osteoporosis [34–37]. Interestingly, *Eno2* knockdown induced significant expression decrease of *Mxi1* (Fig. 5a). Meanwhile, significant correlation (Spearman's ρ 0.67975; *P* value 0.04397) between the expression of *Eno2* and *Mxi1* indicated a positive co-expression between *Eno2* and *Mxi1* (Fig. 6). Therefore, our findings suggested a potential role of *Eno2* in the mechano-transduction for regulation of SOST, which is worthy of further study to confirm.

Sodium/myo-inositol transporter 1 (SMIT1), encoded by Slc5a3, is the major cotransporter for Myo-Inositol (MI), a crucial constituent and nutrient for living cells. I(1,4,5) P_3-mediated Ca^{2+} signaling, a pathway related to MI, was shown to modulate mechanical sensing in osteoblasts in a previous study [38]. SMIT1 knockout mice showed delayed embryonic bone formation, shortened adult long bones, a reduced bone mass, decreased numbers of osteoblasts, and osteoporosis-like microarchitecture, which suggests that SMIT1 plays essential roles in osteogenesis, bone formation, and bone mineral density [39].

B-cell lymphoma 2 (Bcl-2)/adenovirus E1B 19-kDa-interacting protein 3 (BNIP3), encoded by Bnip3, is a member of the apoptotic Bcl-2 protein family, which is involved in the atypical programmed cell death pathway through its modulation of the permeability state of the outer mitochondrial membrane [40]. The upregulation of BNIP3 was shown to contribute to the death of nucleus pulposus cells, which are embedded in intervertebral discs, during disc degeneration [41, 42]. Although most of these key DEGs (Mxi1, Slc5a3, Bnip3, Egln1, Pdk1) showed their important roles in the regulation of bone development, modeling and remodeling, the other key DEGs—specifically, Eno2, Higd1a and Ccng2, which are involved in energy metabolism, cell survival under stress and the regulation of cell cycle, respectively—have not received enough attention in the field of bone research.

It is generally accepted that after differentiation, bone marrow mesenchymal stem cells (MSCs) become lineage-restricted and the terminal differentiated cell type (e.g., osteocyte) becomes irreversible. However, a previous study showed that after 24 h of treatment with parathyroid hormone (PTH), the expression levels of *Kera* (osteoblast

marker) and *E11* (early osteocyte marker) were increased, whereas the expression levels of *Dmp1*, *Phex*, *Mepe* and *Sost* (mature osteocyte marker) were decreased in both mature IDG-SW3 osteocytes and the primary bone osteocytes ex vivo, indicating the loss of differentiation by osteocytes in response to PTH [43]. Their study also showed that some cell cycle-related genes (e.g., Rb1, Cebpa, Hpgd, Nupr1, and Bmp4) showed a decreased expression in response to PTH.

A previous study showed that adipogenic-differentiated cells from ex vivo human MSCs could be dedifferentiated and transdifferentiated into osteogenic or chondrogenic lineage cells, and this procedure is—at least in part—associated with genes associated with cell cycle arrest and progression [44]. Moreover, PTH has also been reported to induce the downregulation of Dmp1 in osteocytes in vivo [45]. Taken together, evidence showed the possible dedifferentiation of osteocytes, which may be associated with the regulation of cell cycle. The results of the present study showed the mechano-sensitive expression of Ccng2, which plays a role in the negative regulation of cell cycle progression.

HIG1 domain family 1A (HIGD1A), which is encoded by Higd1a, is a protein that promotes mitochondrial homeostasis and the survival of cells under stress by inhibiting cytochrome C release and caspase activity [46, 47]. It plays a very important protective effect that saves organs like the heart and brain from hypoxia-related disease [47]. Decreased expression of *Higd1a* by *Eno2* knockdown and correlated expression between them might indicate that *Eno2* may be involved in the hypoxic response of osteocytes.

Gamma-enolase, encoded by Eno2, is a conserved glycolytic enzyme that catalyzes the formation of phosphoenolpyruvate from 2-phosphoglycerate, which generates ATP during glycolysis. A recent study showed that alpha-enolase regulates the AMPK/mTOR pathway, which plays important roles in bone metabolism [48–50], via the concentration of ATP in colorectal cancer cells [51]. Notably, *Eno2* was significantly increased in both human periodontal ligament (PDL) cells with compressive stress [52] and murine osteoblasts with thapsigargin treatment (ER stress) [53].

Mechano-transduction in osteocytes possibly regulates the innervation of bone

Although there have been numerous studies of the key DEGs in the field of bone research, the biological function of these key DEGs in osteocytes has been poorly studied. Thus, to investigate the biological function of the key DEGs, we selectively downregulated the hub gene of the final PPI network using siRNA.

Eno2 knockdown results in a significant increase in the expression of *Gap43* (Fig. 5a). Gap43 encodes the neuromodulin that plays a role in axonal and dendritic filopodia induction. Neuromodulin has been identified in the extracellular vesicles (EVs) derived from human MSCs [54]. Furthermore, the rapid expansion of a dense network of sensory nerve fibers is observed during fracture repair in the periosteum of adult rodents. Thus, it is possible that the induction of nerve fibers is subject to regulation by Gap43 in EVs secreted by osteocytes [55–57]. Interestingly, in the in vitro experiment, the expression of Eno2 and Gap43 did not show a significant correlation under 2.5 dyn/cm^2, while they were highly correlated (Fig. 6) under extremely high mechanical force (50 dyn/cm^2). The co-expression of Eno2 and Gap43 under a pathological force load is consistent with our hypothesis that osteocytes may have able to induct the expansion of nerve fibers under serious injury. However, further physiological studies are necessary to prove this hypothesis. In recent years, there is increasing evidence to support the role of EVs in bone remodeling, and that bone marrow stem cells, osteoblasts, osteoclasts, and osteocytes can communicate with one another and even other types of organs/cells via EVs [58]. Notably, mechanical stimulation has been shown to upregulate the production of EVs in osteocytes, which could enhance bone formation [59], while the muscle cells secreted myostatin downregulate the miR-218 (a microRNA) in EVs derived from osteocytes, which inhibits osteoblastic differentiation [59]. Moreover, previous studies have suggested that some of the regenerative effects are mediated by EVs derived from MSCs [60–62].

Fig. 4 The expression of key candidate DEGs and RANKL & OPG under different force-direction with 50 dyn/cm^2 or under different force-strength with shear stress from 2.5 dyn/cm^2 to 50 dyn/cm^2. (#, Holm–Sidak post hoc test in a one-way ANOVA; $^{\#}P < .05$; $^{\#\#}P < .01$; $^{\#\#\#}P < .001$; $^{\#\#\#\#}P < .0001$. All values represent the mean ± standard deviation)

Summary

In the present study, we screened out and primarily validated some candidate genes that showed extremely mechano-sensitive expression levels. The results indicated the important role of these genes in osteocytes in relation to sensing, recognizing and the differential responses to different types of mechanical stimuli. We also reviewed the previous studies of these genes in the field of bone research. Our research raised a number of questions.

Unloading [63], aging [64], compressive force [65], and osteoporosis [66] could induce the death of osteocytes, while could Higd1a promote osteocyte survival under those conditions? Is it possible that osteocyte-secreted EVs are important for regulating bone metabolism and crosstalk with other organs? Do the cell cycle-related genes play a role such as

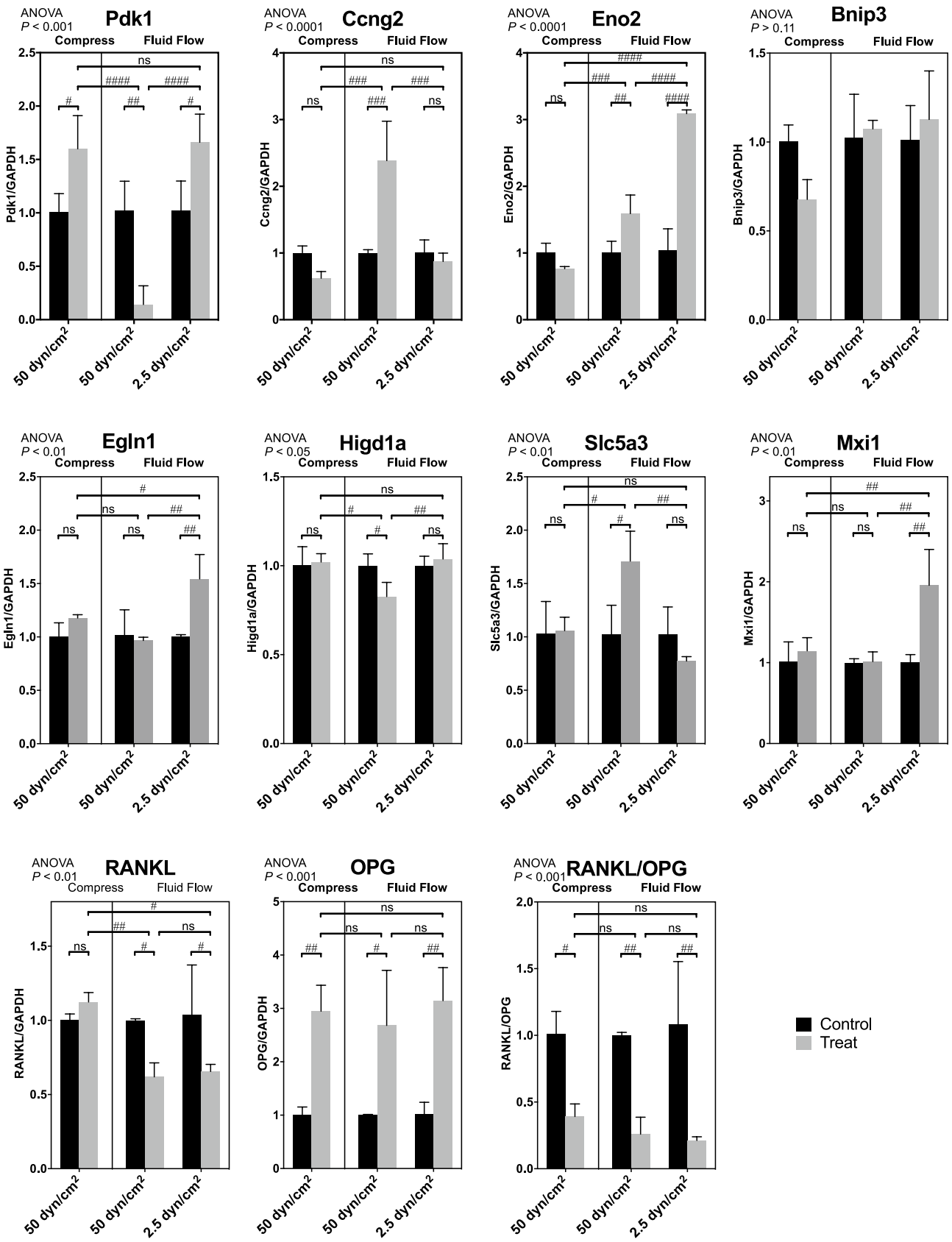
ANOVA
P < 0.001
Pdk1
Compress
Fluid Flow
Pdk1/GAPDH
ANOVA
P < 0.0001
Ccng2
Ccng2/GAPDH
ANOVA
P < 0.0001
Eno2
Eno2/GAPDH
ANOVA
P > 0.11
Bnip3
Bnip3/GAPDH
ANOVA
P < 0.01
Egln1
Egln1/GAPDH
ANOVA
P < 0.05
Higd1a
Higd1a/GAPDH
ANOVA
P < 0.01
Slc5a3
Slc5a3/GAPDH
ANOVA
P < 0.01
Mxi1
Mxi1/GAPDH
ANOVA
P < 0.01
RANKL
RANKL/GAPDH
ANOVA
P < 0.001
OPG
OPG/GAPDH
ANOVA
P < 0.001
RANKL/OPG
RANKL/OPG
50 dyn/cm2
50 dyn/cm2
2.5 dyn/cm2
Control
Treat

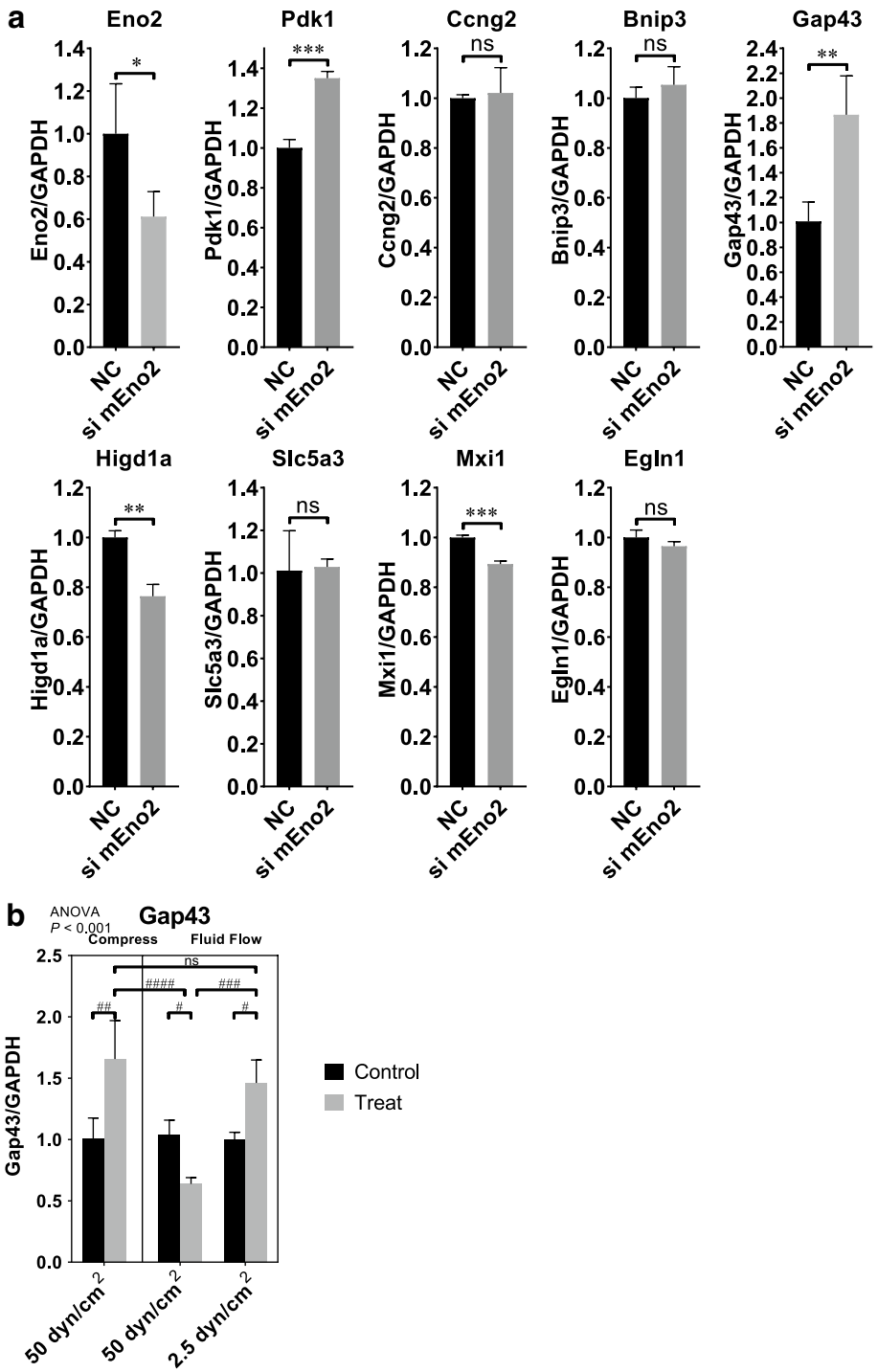

Fig. 5 Results of Eno2 knockdown. **a** The siRNA of *Eno2* significantly reduced the expression of Eno2, Higd1a and Mxi1 while significantly increased the expression of Pdk1 and Gap43. (*, unpaired *t*-test; *, $P < .05$; **, $P < .01$; NC, negative control; si mEno2, Eno2 siRNA). **b** The expression of Gap43 in normal cells under different force-direction or force-strength conditions (#, Holm–Sidak post hoc test in a one-way ANOVA; $^{\#}P < .05$; $^{\#\#}P < .01$; $^{\#\#\#}P < .001$; $^{\#\#\#\#}P < .0001$). (all values represent the mean ± standard deviation)

triggering dedifferentiation of osteocytes? How exactly do the key DEGs that we screened out regulate the osteocyte functions? What is the exact mechanism of the mechanosensitive expression of these key DEGs? Some of these questions have touched on some current topics in the field of bone research. Other questions are related to genes that have not been completely studied; thus, their relationship to bone remains unclear. The authors believe that exploring and finally answering these questions could improve our understanding of mechano-transduction in osteocytes and may lead to the development of new therapeutic agents for bone diseases.

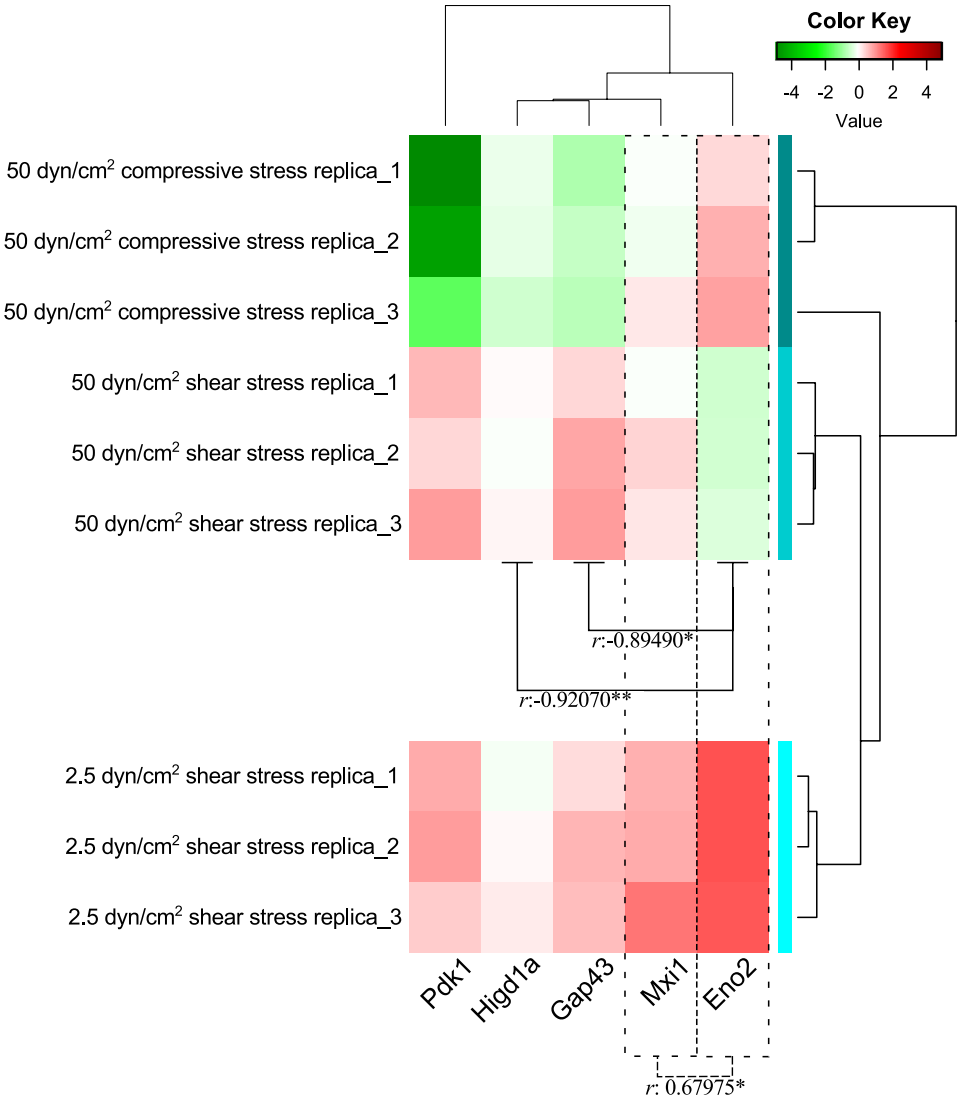

Fig. 6 We converted the results from both Figs. 4 and 5b to create a heatmap with Pearson correlation test to investigate the correlation of the Eno2 and expression of other genes (Pdk1, Higd1a, Mxi1, and Gap43) under different force-direction or force-strength conditions. (*r*, Pearson correlation coefficient; *, $P < .05$; **, $P < .01$)

Acknowledgements The present work was supported by Grant-in-Aid for Scientific Research (to H. Kamioka [16H05549] and [16K15837], to Y. Ishihara [17H04413]) from the Japan Society for the Promotion of Science, Japan. Lastly, Ziyi Wang would like to dedicate this article to his wife, Yao Weng, who saw too much of the back of his head as he looked at the computer screen while he was coding, processing data and revising the manuscript before the deadline. His wife's tolerance is best described as remarkable.

Compliance with ethical standards

Conflict of interest All authors have no conflicts of interest.

References

1. Galea GL, Lanyon LE, Price JS (2017) Sclerostin's role in bone's adaptive response to mechanical loading. Bone 96:38–44. https://doi.org/10.1016/j.bone.2016.10.008
2. Sugawara Y, Kamioka H, Ishihara Y et al (2013) The early mouse 3D osteocyte network in the presence and absence of mechanical loading. Bone 52:189–196. https://doi.org/10.1016/j.bone.2012.09.033
3. Weinbaum S, Cowin SC, Zeng Y (1994) A model for the excitation of osteocytes by mechanical loading-induced bone fluid shear stresses. J Biomech 27:339–360. https://doi.org/10.1016/0021-9290(94)90010-8
4. Adachi T, Aonuma Y, Ito Ichi S et al (2009) Osteocyte calcium signaling response to bone matrix deformation. J Biomech 42:2507–2512. https://doi.org/10.1016/j.jbiomech.2009.07.006
5. Sapir-Koren R, Livshits G (2014) Osteocyte control of bone remodeling: is sclerostin a key molecular coordinator of the balanced bone resorption–formation cycles? Osteoporos Int 25:2685–2700. https://doi.org/10.1007/s00198-014-2808-0
6. Kamioka H, Honjo T, Takano-Yamamoto T (2001) A three-dimensional distribution of osteocyte processes revealed by the combination of confocal laser scanning microscopy and differential interference contrast microscopy. Bone 28:145–149. https://doi.org/10.1016/S8756-3282(00)00421-X
7. Jing D, Baik AD, Lu XL et al (2014) In situ intracellular calcium oscillations in osteocytes in intact mouse long bones under

dynamic mechanical loading. FASEB J 28:145–149. https://doi.org/10.1096/fj.13-237578
8. Phipson B, Lee S, Majewski IJ et al (2016) Robust hyperparameter estimation protects against hypervariable genes and improves power to detect differential expression. Ann Appl Stat 10:946–963. https://doi.org/10.1214/16-AOAS920
9. Ashburner M, Ball CA, Blake JA et al (2000) Gene Ontology: tool for the unification of biology. Nat Genet 25:25–29. https://doi.org/10.1038/75556
10. Carbon S, Dietze H, Lewis SE et al (2017) Expansion of the Gene Ontology knowledgebase and resources. Nucleic Acids Res 45:D331–D338. https://doi.org/10.1093/nar/gkw1108
11. Ogata H, Goto S, Sato K et al (1999) KEGG: kyoto encyclopedia of genes and genomes. Nucleic Acids Res 27:29–34. https://doi.org/10.1093/nar/27.1.29
12. Huang D, Sherman BT, Tan Q et al (2007) The DAVID gene functional classification tool: a novel biological module-centric algorithm to functionally analyze large gene lists. Genome Biol 8:R183. https://doi.org/10.1186/gb-2007-8-9-r183
13. Mering C v (2003) STRING: a database of predicted functional associations between proteins. Nucleic Acids Res 31:258–261. https://doi.org/10.1093/nar/gkg034
14. Kohl M, Wiese S, Warscheid B (2011) Cytoscape: software for visualization and analysis of biological networks. In: Hamacher M, Eisenacher M, Stephan C (eds) Data mining in proteomics: from standards to applications, 1st edn. Springer, Heidelberg, pp 291–303
15. Yip KY, Yu H, Kim PM et al (2006) The tYNA platform for comparative interactomics: a web tool for managing, comparing and mining multiple networks. Bioinformatics 22:2968–2970. https://doi.org/10.1093/bioinformatics/btl488
16. Kamioka H, Sugawara Y, Murshid SA et al (2006) Fluid shear stress induces less calcium response in a single primary osteocyte than in a single osteoblast: implication of different focal adhesion formation. J Bone Miner Res 21:1012–1021. https://doi.org/10.1359/jbmr.060408
17. Frangos J, Eskin S, McIntire L, Ives C (1985) Flow effects on prostacyclin production by cultured human endothelial cells. Science 227:1477–1479. https://doi.org/10.1126/science.3883488
18. Odagaki N, Ishihara Y, Wang Z et al (2018) Role of osteocyte-PDL crosstalk in tooth movement via SOST/sclerostin. J Dent Res. https://doi.org/10.1177/0022034518771331
19. Yu K, Sellman DP, Bahraini A et al (2017) Mechanical loading disrupts osteocyte plasma membranes which initiates mechanosensation events in bone. J Orthop Res 36:653–662. https://doi.org/10.1002/jor.23665
20. Wu C, Rankin EB, Castellini L et al (2015) Oxygen-sensing PHDs regulate bone homeostasis through the modulation of osteoprotegerin. Genes Dev 29:817–831. https://doi.org/10.1101/gad.255000.114
21. Shen X, Wan C, Ramaswamy G et al (2009) Prolyl hydroxylase inhibitors increase neoangiogenesis and callus formation following femur fracture in mice. J Orthop Res 27:1298–1305. https://doi.org/10.1002/jor.20886
22. Huang J, Liu L, Feng M et al (2015) Effect of CoCl2 on fracture repair in a rat model of bone fracture. Mol Med Rep 12:5951–5956. https://doi.org/10.3892/mmr.2015.4122
23. Stewart R, Goldstein J, Eberhardt A et al (2011) Increasing vascularity to improve healing of a segmental defect of the rat femur. J Orthop Trauma 25:472–476. https://doi.org/10.1097/BOT.0b013e31822588d8
24. Zhang W, Li G, Deng L et al (2012) New bone formation in a true bone ceramic scaffold loaded with desferrioxamine in the treatment of segmental bone defect: a preliminary study. J Orthop Sci 17:289–298. https://doi.org/10.1007/s00776-012-0206-z
25. Wan C, Gilbert SR, Wang Y et al (2008) Activation of the hypoxia-inducible factor-1 pathway accelerates bone regeneration. Proc Natl Acad Sci 105:686–691. https://doi.org/10.1073/pnas.0708474105
26. Liu X, Tu Y, Zhang L et al (2014) Prolyl hydroxylase inhibitors protect from the bone loss in ovariectomy rats by increasing bone vascularity. Cell Biochem Biophys 69:141–149. https://doi.org/10.1007/s12013-013-9780-8
27. Peng J, Lai ZG, Fang ZL et al (2014) Dimethyloxalylglycine prevents bone loss in ovariectomized C57BL/6 J mice through enhanced angiogenesis and osteogenesis. PLoS One 9:e112744. https://doi.org/10.1371/journal.pone.0112744
28. Bentovim L, Amarilio R, Zelzer E (2013) HIF1 is a central regulator of collagen hydroxylation and secretion under hypoxia during bone development. Development 140:248–248. https://doi.org/10.1242/dev.092023
29. Kim J, Tchernyshyov I, Semenza GL, Dang CV (2006) HIF-1-mediated expression of pyruvate dehydrogenase kinase: a metabolic switch required for cellular adaptation to hypoxia. Cell Metab 3:177–185. https://doi.org/10.1016/j.cmet.2006.02.002
30. Wenger RH, Stiehl DP, Camenisch G (2005) Integration of oxygen signaling at the consensus HRE. Sci Signal 2005:re12–re12. https://doi.org/10.1126/stke.3062005re12
31. Fujiwara M, Kubota T, Wang W et al (2016) Successful induction of sclerostin in human-derived fibroblasts by 4 transcription factors and its regulation by parathyroid hormone, hypoxia, and prostaglandin E2. Bone 85:91–98. https://doi.org/10.1016/j.bone.2016.01.024
32. Lin C, Jiang X, Dai Z et al (2009) Sclerostin mediates bone response to mechanical unloading through antagonizing wnt/β-catenin signaling. J Bone Miner Res 24:1651–1661. https://doi.org/10.1359/jbmr.090411
33. Winkler DG (2003) Osteocyte control of bone formation via sclerostin, a novel BMP antagonist. EMBO J 22:6267–6276. https://doi.org/10.1093/emboj/cdg599
34. Ellies DL, Viviano B, McCarthy J et al (2006) Bone density ligand, sclerostin, directly interacts with LRP5 but not LRP5G171 V to modulate wnt activity. J Bone Miner Res 21:1738–1749. https://doi.org/10.1359/jbmr.060810
35. McGee-Lawrence ME, Ryan ZC, Carpio LR et al (2013) Sclerostin deficient mice rapidly heal bone defects by activating β-catenin and increasing intramembranous ossification. Biochem Biophys Res Commun 441:886–890. https://doi.org/10.1016/j.bbrc.2013.10.155
36. Cosman F, Crittenden DB, Adachi JD et al (2016) Romosozumab treatment in postmenopausal women with osteoporosis. N Engl J Med 375:1532–1543. https://doi.org/10.1056/NEJMoa1607948
37. Saag KG, Petersen J, Brandi ML et al (2017) Romosozumab or alendronate for fracture prevention in women with osteoporosis. N Engl J Med 377:1417–1427. https://doi.org/10.1056/NEJMoa1708322
38. Chen NX, Ryder KD, Pavalko FM et al (2000) Ca^{2+} regulates fluid shear-induced cytoskeletal reorganization and gene expression in osteoblasts. Am J Physiol Cell Physiol 278:C989–C997. https://doi.org/10.1152/ajpcell.2000.278.5.C989
39. Dai Z, Chung SK, Miao D et al (2011) Sodium/myo-inositol cotransporter 1 and myo-inositol are essential for osteogenesis and bone formation. J Bone Miner Res 26:582–590. https://doi.org/10.1002/jbmr.240
40. Vande Velde C, Cizeau J, Dubik D et al (2000) BNIP3 and genetic control of necrosis-like cell death through the mitochondrial permeability transition pore. Mol Cell Biol 20:5454–5468. https://doi.org/10.1128/MCB.20.15.5454-5468.2000
41. Liu J, Yuan C, Pu L, Wang J (2017) Nutrient deprivation induces apoptosis of nucleus pulposus cells via activation of the BNIP3/

AIF signalling pathway. Mol Med Rep 16:7253–7260. https://doi.org/10.3892/mmr.2017.7550
42. Liu J, Wang J, Zhou Y (2012) Upregulation of BNIP3 and translocation to mitochondria in nutrition deprivation induced apoptosis in nucleus pulposus cells. Jt Bone Spine 79:186–191. https://doi.org/10.1016/j.jbspin.2011.04.011
43. Prideaux M, Dallas SL, Zhao N et al (2015) Parathyroid hormone induces bone cell motility and loss of mature osteocyte phenotype through L-calcium channel dependent and independent mechanisms. PLoS ONE 10:1–25. https://doi.org/10.1371/journal.pone.0125731
44. Ullah M, Stich S, Notter M et al (2013) Transdifferentiation of mesenchymal stem cells-derived adipogenic-differentiated cells into osteogenic- or chondrogenic-differentiated cells proceeds via dedifferentiation and have a correlation with cell cycle arresting and driving genes. Differentiation 85:78–90. https://doi.org/10.1016/j.diff.2013.02.001
45. Bellido T, Ali AA, Gubrij I et al (2005) Chronic elevation of parathyroid hormone in mice reduces expression of sclerostin by osteocytes: a novel mechanism for hormonal control of osteoblastogenesis. Endocrinology 146:4577–4583. https://doi.org/10.1210/en.2005-0239
46. Ameri K, Rajah AM, Nguyen V et al (2013) Nuclear localization of the mitochondrial factor HIGD1A during metabolic stress. PLoS One 8:e62758. https://doi.org/10.1371/journal.pone.0062758
47. An HJ, Shin H, Jo SG et al (2011) The survival effect of mitochondrial Higd-1a is associated with suppression of cytochrome C release and prevention of caspase activation. Biochim Biophys Acta-Mol Cell Res 1813:2088–2098. https://doi.org/10.1016/j.bbamcr.2011.07.017
48. Yokomoto-Umakoshi M, Kanazawa I, Takeno A et al (2016) Activation of AMP-activated protein kinase decreases receptor activator of NF-κB ligand expression and increases sclerostin expression by inhibiting the mevalonate pathway in osteocytic MLO-Y4 cells. Biochem Biophys Res Commun 469:791–796. https://doi.org/10.1016/j.bbrc.2015.12.072
49. Tascau L, Gardner T, Anan H et al (2016) Activation of protein kinase a in mature osteoblasts promotes a major bone anabolic response. Endocrinology 157:112–126. https://doi.org/10.1210/en.2015-1614
50. Takeno A, Kanazawa I, Tanaka K et al (2015) Activation of AMP-activated protein kinase protects against homocysteine-induced apoptosis of osteocytic MLO-Y4 cells by regulating the expressions of NADPH oxidase 1 (Nox1) and Nox2. Bone 77:135–141. https://doi.org/10.1016/j.bone.2015.04.025
51. Zhan P, Zhao S, Yan H et al (2017) α-enolase promotes tumorigenesis and metastasis via regulating AMPK/mTOR pathway in colorectal cancer. Mol Carcinog 56:1427–1437. https://doi.org/10.1002/mc.22603
52. de Araujo RMS, Oba Y, Moriyama K (2007) Identification of genes related to mechanical stress in human periodontal ligament cells using microarray analysis. J Periodontal Res 42:15–22. https://doi.org/10.1111/j.1600-0765.2006.00906.x
53. Hamamura K, Liu Y, Yokota H (2008) Microarray analysis of thapsigargin - Induced stress to the endoplasmic reticulum of mouse osteoblasts. J Bone Miner Metab 26:231–240. https://doi.org/10.1007/s00774-007-0825-1
54. Kim H-S, Choi D-Y, Yun SJ et al (2012) Proteomic analysis of microvesicles derived from human mesenchymal stem cells. J Proteome Res 11:839–849. https://doi.org/10.1021/pr200682z
55. Li J, Ahmad T, Spetea M et al (2001) Bone reinnervation after fracture: a study in the rat. J Bone Miner Res 16:1505–1510. https://doi.org/10.1359/jbmr.2001.16.8.1505
56. Strange-Vognsen HH, Laursen H (1997) Nerves in human epiphyseal uncalcified cartilage. J Pediatr Orthop B 6:56–58
57. Hukkanen M, Konttinen YT, Santavirta S et al (1993) Rapid proliferation of calcitonin gene-related peptide-immunoreactive nerves during healing of rat tibial fracture suggests neural involvement in bone growth and remodelling. Neuroscience 54:969–979. https://doi.org/10.1016/0306-4522(93)90588-7
58. Liu M, Sun Y, Zhang Q (2018) Emerging role of extracellular vesicles in bone remodeling. J Dent Res. https://doi.org/10.1177/0022034518764411
59. Qin Y, Peng Y, Zhao W et al (2017) Myostatin inhibits osteoblastic differentiation by suppressing osteocyte-derived exosomal microRNA-218: a novel mechanism in muscle-bone communication. J Biol Chem 292:11021–11033. https://doi.org/10.1074/jbc.M116.770941
60. Herrera MB, Fonsato V, Gatti S et al (2010) Human liver stem cell-derived microvesicles accelerate hepatic regeneration in hepatectomized rats. J Cell Mol Med 14:1605–1618. https://doi.org/10.1111/j.1582-4934.2009.00860.x
61. Lai RC, Arslan F, Lee MM et al (2010) Exosome secreted by MSC reduces myocardial ischemia/reperfusion injury. Stem Cell Res 4:214–222. https://doi.org/10.1016/j.scr.2009.12.003
62. Bruno S, Grange C, Deregibus MC et al (2009) Mesenchymal stem cell-derived microvesicles protect against acute tubular injury. J Am Soc Nephrol 20:1053–1067. https://doi.org/10.1681/ASN.2008070798
63. Aguirre JI, Plotkin LI, Stewart SA et al (2006) Osteocyte apoptosis is induced by weightlessness in mice and precedes osteoclast recruitment and bone loss. J Bone Miner Res 21:605–615. https://doi.org/10.1359/jbmr.060107
64. Manolagas SC, Parfitt AM (2010) What old means to bone. Trends Endocrinol Metab 21:369–374. https://doi.org/10.1016/j.tem.2010.01.010
65. Takano-Yamamoto T (2014) Osteocyte function under compressive mechanical force. Jpn Dent Sci Rev 50:29–39. https://doi.org/10.1016/j.jdsr.2013.10.004
66. Plotkin LI (2014) Apoptotic osteocytes and the control of targeted bone resorption. Curr Osteoporos Rep 12:121–126. https://doi.org/10.1007/s11914-014-0194-3